

Introduction of Novel Substrate Oxidation into Cytochrome *c* Peroxidase by Cavity Complementation: Oxidation of 2-Aminothiazole and Covalent Modification of the Enzyme^{†,‡}

Rabi A. Musah and David B. Goodin*

Department of Molecular Biology, MB8, The Scripps Research Institute, 10550 North Torrey Pines Road, La Jolla, California 92037

Received April 7, 1997; Revised Manuscript Received July 14, 1997[⊗]

ABSTRACT: The binding and oxidation of an artificial substrate, 2-aminothiazole, by an engineered cavity of cytochrome *c* peroxidase is described. The W191G mutant has been shown to create a buried cavity into which a number of small heterocyclic compounds will bind [Fitzgerald, M. M., Churchill, M. J., McRee, D. E., & Goodin, D. B. (1994) *Biochemistry* 33, 3807–3818], providing a specific site near the heme from which substrates might be oxidized. In this study, we show by titration calorimetry that 2-aminothiazole binds to W191G with a K_d of 0.028 mM at pH 6. A crystal structure at 2.3 Å resolution of W191G in the presence of 2-aminothiazole reveals the occupation of this compound in the cavity, and indicates that it is in van der Waals contact with the heme. The WT enzyme reacts with H₂O₂ to form Compound ES, in which both the iron center and the Trp-191 side chain are reversibly oxidized. For the W191F (and perhaps the W191G) mutants, the iron is still oxidized, but the second equivalent exists transiently as a radical on the porphyrin before migrating to an alternate protein radical site [Erman, J. E., Vitello, L. B., Mauro, J. M., & Kraut, J. (1989) *Biochemistry* 28, 7992–7995]. Two separate reactions are observed between 2-aminothiazole and the oxidized centers of W191G. In the one reaction, optical and EPR spectra of the heme are used to show that 2-aminothiazole acts as an electron donor to the ferryl (Fe⁴⁺=O) center of W191G to reduce it to the ferric oxidation state. This reaction occurs from within the cavity, as it is not observed for variants that lack this artificial binding site. A second reaction between 2-aminothiazole and peroxide-oxidized W191G, which is much less efficient, results in the specific covalent modification of Tyr-236. Electrospray mass spectra of the W191G after incubation in 2-aminothiazole and H₂O₂ show a modification of the protein indicative of covalent binding of 2-aminothiazole. The site of modification was determined to be Tyr-236 by CNBr peptide mapping and automated peptide sequencing. The covalent modification is only observed for W191G and W191F which form the alternate radical center. This observation provides an unanticipated assignment of this free radical species to Tyr-236, which is consistent with previous proposals that it is a tyrosine. The oxidation of 2-aminothiazole by W191G represents an example of how the oxidative capacity inherent in the heme prosthetic group and the specific binding behavior of artificial protein cavities can be harnessed and redirected toward the oxidation of organic substrates.

The results of recent studies suggest that the method of cavity complementation for introducing small molecule binding sites into proteins might be successfully employed for the design of artificial enzymes capable of recognition and chemical transformation of unnatural substrates. Deletions of an amino acid side chain from the interior of several protein structures have resulted in uncollapsed cavities that retain the shape, hydrogen bonding potential, and hydrophobicity/polarity of the surrounding environment, allowing the binding of small exogenous ligands (Barrick, 1994; Depillis et al., 1994; Eriksson et al., 1992; Fitzgerald et al., 1994; McRee et al., 1994; Morton et al., 1995; Morton & Mathews, 1995). Although binding sites with reasonable specificity can be introduced into protein structures in this

way, inducing enzyme catalysis as a result is a much more formidable task since transition state stability is extremely sensitive to the exact positioning of chemical functionalities between enzyme and substrate for most chemical transformations. However, certain types of enzymatic activity may be achieved with this method if a system is chosen in which the most important factor for the reaction is the degree of access of a potential substrate to a preexisting catalytic framework exhibiting broad specificity.

An attractive target for such an engineered enzyme is yeast cytochrome *c* peroxidase (CCP)¹ because of the way this enzyme stores and utilizes its oxidizing potential. CCP catalyzes the oxidation of two molecules of ferrocytochrome *c* (cyt *c*) (Scheme 1) by H₂O₂ in yeast mitochondria (Poulos & Finzel, 1984; Yonetani, 1976). It is a general property of heme peroxidases that they react with H₂O₂ to form a two-electron-oxidized state, normally referred to as Compound I, containing an oxyferryl iron center (Fe⁴⁺=O) and a porphyrin π cation radical (Dolphin et al., 1971). However, the analogous state of CCP, Compound ES, is unusual in that the second oxidizing equivalent exists as a cation radical

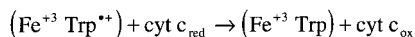
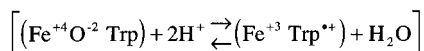
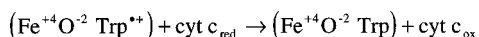
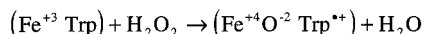
[†] This research was supported by Grants GM-41049 to D.B.G. and GM-17844 to R.A.M. from the NIH.

[‡] The crystallographic coordinates for the structure presented in this work have been deposited with the Protein Data Bank, Chemistry Department, Brookhaven National Laboratory, Upton, NY 11973, from which copies are available (entry 1aev).

* Author to whom correspondence should be addressed.

[⊗] Abstract published in *Advance ACS Abstracts*, September 15, 1997.

Scheme 1



on the Trp-191 side chain instead of the porphyrin (Scheme 1) (Erman et al., 1989; Houseman et al., 1993; Huyett et al., 1995; Sivaraja et al., 1989). Once oxidized, the Trp-191 cation radical is stabilized electrostatically by several interactions with the protein, including the buried carboxylate of Asp-235 (Fitzgerald et al., 1995) and the peptide carbonyl moieties of Leu-177 and His-175 (Miller et al., 1994) (Figure 1). These interactions may also determine that Trp-191 specifically is oxidized over other nearby tyrosines, tryptophans, and methionines. It therefore appears that the protein structure surrounding the Trp-191 side chain has been ideally evolved to promote the oxidation of this specific indole side chain, and for this reason, CCP may be thought to catalyze the oxidation of this residue as an internal, covalently bound pseudosubstrate.

It is likely that the Trp-191 side chain is oxidized by an initially formed intermediate similar to Compound I consisting of both ferryl heme and a porphyrin radical. While this initial intermediate has not been seen directly in the wild type (WT) enzyme, it has been detected as a transient species after peroxide oxidation of the W191F mutant (Erman et al., 1989). W191F reacts with H_2O_2 to give a two-electron-oxidized species with the optical spectrum of Compound I. However, in the absence of Trp-191, this unstable porphyrin radical decays within about 50 ms and an alternate free radical species is formed in substoichiometric amounts (Erman et al., 1989; Fishel et al., 1991; Scholes et al., 1989). The narrow isotropic EPR signals observed for this alternate radical have g values and proton hyperfine structure that are similar to those observed for other tyrosine radicals (Gerfen et al., 1993; Hoganson & Babcock, 1992; Warncke et al., 1994), supporting the proposal that this narrow signal is associated with a Tyr residue (Fishel et al., 1991; Hori & Yonetani, 1985). However, the exact identity of this alternate radical site remains unknown. Thus, the peroxide-oxidized state of CCP contains two oxidizing centers, ferryl heme and Trp-191 radical, while the oxidized state of mutants, such as W191F and presumably also W191G, contains a ferryl heme and an unstable porphyrin radical that rapidly oxidizes an alternate protein site.

We have shown previously that the W191G mutant of CCP contains a buried polar cavity at the site of the tryptophan

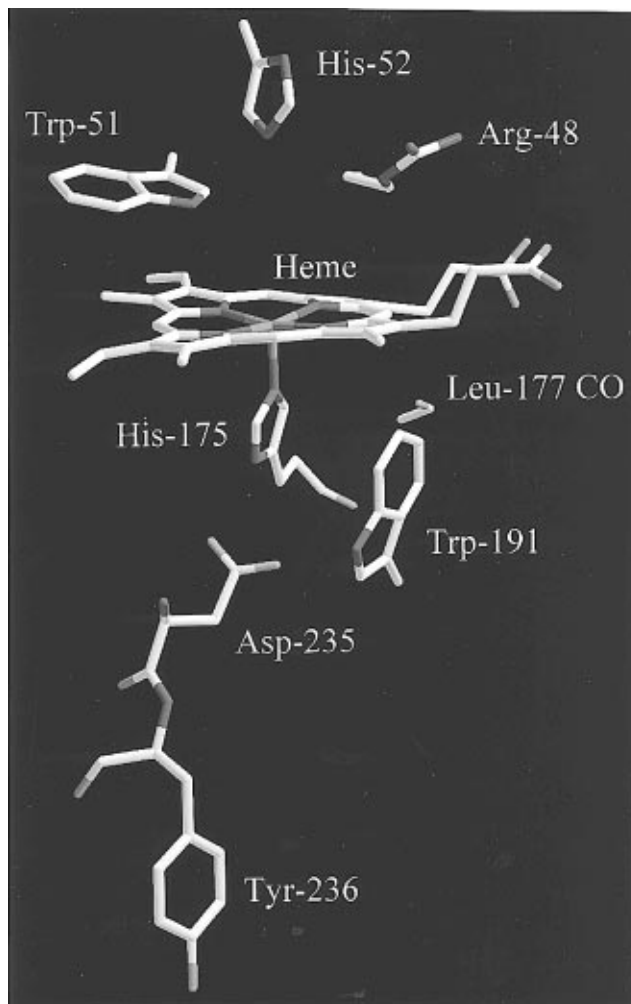


FIGURE 1: Structure surrounding the Trp radical site of cytochrome *c* peroxidase. Asp-235 and the peptide carbonyl oxygens of Leu-177 and His-175 stabilize the Trp radical cation and determine the cation specificity for ligands which bind to the cavity formed by deletion of Trp-191.

side chain (Fitzgerald et al., 1994), which was shown to readily bind a number of small cationic imidazoles. While imidazoles themselves are not easily oxidized, other compounds that bind to this site might react with the oxidized heme by a mechanism analogous to that observed for Trp-191 in the native enzyme. The same interactions that stabilize the formation of the cation radical of Trp-191 would also stabilize the transition state for electron withdrawal from a surrogate substrate. In this paper, we describe the binding of 2-aminothiazole (2AT), within the W191G cavity. Further, we show that this compound undergoes two separate reactions with the oxidized centers of W191G, one with the heme and one with a specific tyrosine residue. The reaction with the heme indicates direct electron donation from within the artificial binding site, and the modification of Tyr-236 provides an assignment of the alternate radical species.

MATERIALS AND METHODS

CCP Expression and Purification from Escherichia coli. The W191G mutant of CCP was constructed by site-directed mutagenesis, overexpressed in *E. coli* BL21(DE3), and purified as previously described (Fitzgerald et al., 1994).

¹ Abbreviations: CCP, cytochrome *c* peroxidase; CCP(MKT), cytochrome *c* peroxidase produced by expression in *Escherichia coli* containing Met-Lys-Thr at the N terminus, Ile at position 53, and Gly at position 152; cyt *c*, cytochrome *c*; EPR, electron paramagnetic resonance; Compound ES, H_2O_2 -oxidized state of CCP containing the ferryl and Trp cation radical moieties; Compound I, H_2O_2 -oxidized state of peroxidases containing the ferryl and porphyrin π cation moieties; WT, wild type CCP; W191G, mutant in which Trp-191 is replaced by Gly; W191F, mutant in which Trp-191 is replaced by Phe; 2AT, 2-aminothiazole; TFA, trifluoroacetic acid; CNBr, cyanogen bromide; FAB, fast atom bombardment; EMS, electrospray ionization mass spectrometry; MPD, 2-methyl-2,4-pentandiol.

Measurement of Binding Affinities. Calorimetric experiments were performed using a MC2 titration calorimeter from Microcal, Inc. Experiments were conducted at 25 °C in 100 mM BIS-TRIS propane at pH 6.0. W191G protein solutions with known concentrations (0.2–0.4 mM) were titrated with 5 μ L injections of a solution of 2AT which was at a concentration 10–20 times higher than that of the initial W191G protein solution. Injections were spaced at intervals of approximately 4 min with 400 rpm cell stirring and were continued well past the titration inflection to allow accurate subtraction of the heats of mixing of the two components. Data analysis was performed using the ORIGIN program (Microcal, Inc.) and involved fitting the background-subtracted, integrated heat peaks to an equation describing a single-site binding isotherm, to give association constants, molar enthalpy, and the number of ligands bound per protein. Binding free energies were calculated as $-RT \ln K$, using a 1 M standard state, and binding entropies were calculated as $(\Delta G - \Delta H)/T$.

X-ray Crystallography. Single crystals of X-ray diffraction quality were grown from 25% 2-methyl-2,4-pentanediol (MPD) by vapor diffusion as previously described (Fitzgerald et al., 1994). W191G crystals were soaked for 1 h in 40% MPD, 100 mM potassium phosphate buffer (pH 6.0), and 50 mM 2AT. Room-temperature X-ray diffraction data were collected at 15 °C using CuK α radiation from the rotating anode of a Rigaku X-ray generator and a Siemens area detector. Data were indexed and integrated using the XENGEN programs (Howard et al., 1985). For low-temperature data collection, a suitable W191G crystal was soaked for 1 h in 30% polyethylene glycol, mounted in a loop of human hair, and flash-cooled in the liquid nitrogen boil-off jet. X-ray diffraction data were collected at -180 °C with a low-temperature controller from Area Detector Systems Corp. (ADSC) that is integrated with a Siemens SRA direct drive rotating anode operating at 50 kV and 100 mA (0.3 mm focus) and equipped with a 30 cm Mar image plate. Image plate data were processed using DENZO (Otwinowski, 1993). All data were analyzed by difference Fourier techniques using the Scripps XtalView software (McRee, 1992).

Reactions of 2AT with CCP. 2AT was obtained from Aldrich Chemical Co. UV-vis spectra were collected at 25 °C in 100 mM potassium phosphate at pH 6.0 using a Hewlett-Packard 8452A or 8453 diode array spectrophotometer. Compound ES was formed by adding 1.2 equiv of H₂O₂ to 10 μ M enzyme in 100 mM potassium phosphate at pH 6.0. Stock solutions of 2AT (100 mM) were prepared in 20% ethanol/water. Reductive titration of Compound ES was carried out by adding 1 μ L aliquots of a 2AT stock solution every minute and observing the blue shift in the Compound ES Soret maximum. EPR spectra were collected in 3 mm OD quartz tubes at X-band on a Bruker ESP300 spectrometer at 77 K. The temperature was measured with a GaAs diode calibrated to ± 0.1 K. EPR samples consisted of 900 μ M enzyme in 100 mM potassium phosphate buffer. A spectrum was recorded first for the ferric state. The sample was thawed, and 1.2 equiv of H₂O₂ was added before refreezing and collecting the EPR spectra of the oxidized samples. Reduction of the oxidized ferryl enzyme by 2AT was measured by a series of experiments in which the samples were thawed and 2AT was added with mixing

followed by refreezing and storage of the tubes directly in liquid nitrogen.

Covalent Modification of W191G by 2AT. The reaction of oxidized WT, W191G, and W191F with 2AT was carried out as follows. To 836 μ L of stirred 1 mM aqueous 2AT was added 55 μ L of 3 mM protein in 100 mM potassium phosphate at pH 6.0, followed by 33.4 μ L of 100 mM aqueous H₂O₂. All reactions were carried out at 25 °C. Control experiments were performed identically, except that no 2AT was present. The reactions were allowed to proceed for 3 h with stirring. Each protein sample was then analyzed by HPLC on a Hitachi L-6200A intelligent pump and an L-4200 UV-vis detector, using an analytical Supelcosil LC-18 C₁₈ reversed phase column with a flow rate of 1 mL/min, and detection at 280 nm. Solvent A contained 10% 2-propanol and 90% of a 0.1% solution of trifluoroacetic acid (TFA), and solvent B contained 90% 2-propanol and 10% of a 0.1% aqueous TFA solution. The apoprotein and heme were eluted with a linear gradient from 5 to 70% B over 50 min and analyzed directly by electrospray ionization mass spectrometry (EMS) using an API III Perkin-Elmer SCIEX triple quadrupole mass spectrometer. Samples were introduced into the mass analyzer at a rate of 4 mL/min. The positive and negative ions generated by charged droplet evaporation entered the analyzer through an interface plate and a 100 mm orifice, with a declustering potential of 50–200 V. The emitter voltage was maintained at 5000 V. Protein at concentrations of 150–200 μ M was used in each experiment. As previously noted (Siuzdak, 1994), removal of all salt by HPLC was important in attaining high mass resolution in the range of $\pm 0.01\%$ (± 3 amu for CCP). In practice, our absolute error between the expected and observed mass of WT CCP from multiple determinations of a number of mutant proteins over the course of these experiments was well within this value, and this additional accuracy can possibly be attributed to the extreme protein purity which is possible with multiple rounds of recrystallization.

Peptide Mapping. A stock solution of cyanogen bromide (CNBr, 900 μ L), made by dissolving 0.1145 g of CNBr in 1000 μ L of 0.2 N HCl, was added to the protein solution. The resulting reaction mixture was allowed to stir overnight. The samples were then lyophilized, and the residue taken up in 400 μ L of 0.2 N AcOH. The samples were analyzed by reversed phase HPLC with a flow rate of 1 mL/min and detection at 220 nm. Solvent A contained 0.1% aqueous TFA and solvent B 0.1% TFA in acetonitrile. Peptides were eluted with a linear gradient from 30 to 100% B over 60 min and 100% B for 20 min, followed by a linear gradient to 30% B over 20 min. The peptide fractions were analyzed by EMS and sequenced by the Scripps core facility.

RESULTS

2AT Binds to the W191G Cavity. 2AT was identified as a promising candidate in our search for an artificial substrate for W191G because of its relatively high binding affinity with respect to the W191G cavity and because of its potential to be oxidized by the heme. Previous studies have shown that the W191G cavity binds a number of molecules with better than millimolar affinities provided that they are small (five- or six-membered ring) heterocyclic compounds that carry an overall positive charge (Fitzgerald et al., 1994; R. Musah, unpublished results). In the process of screening

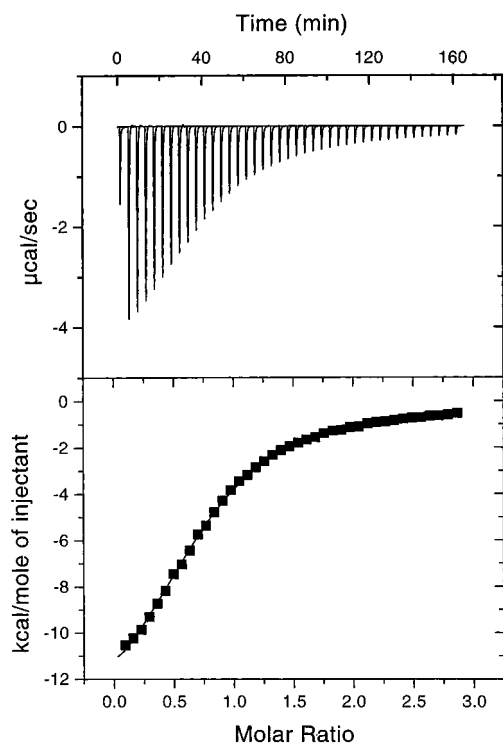


FIGURE 2: Calorimetric titration of W191G with 2AT. Isothermal titration calorimetry profile of W191G titrated with 2AT in 100 mM BIS-TRIS propane at pH 6.0. The upper graph shows the raw data for the heat evolved following each addition of 2AT to the protein in microcalories per second. Shown at the bottom is the corrected integrated area of each peak as a function of molar ratio. The fitted line corresponds to a single-site binding model which gives a K_a of $3.66 \times 10^4 \text{ M}^{-1}$, 0.8 molecule of 2AT bound per site, and a ΔH of -15.2 kcal/mol .

such compounds, we have obtained evidence that 2AT behaves as such a cavity binder.

The binding affinity of 2AT with respect to W191G was measured by titration calorimetry. Titrations of W191G with 2AT at 25 °C in 100 mM BIS-TRIS propane at pH 6.0 gave clear binding isotherms (Figure 2) which were easily fit to a single-site binding model to give a K_d of 0.027 mM and 0.8 molecule of 2AT bound per site. The corresponding thermodynamic parameters calculated from these data for 2AT binding were as follows: $\Delta H = -15.2 \text{ kcal/mol}$, $\Delta S = -30.0 \text{ cal mol}^{-1} \text{ K}^{-1}$, and $\Delta G = -6.20 \text{ kcal/mol}$. Titration of WT and W191F CCP with 2AT gave only small, relatively constant background heat peaks that could not be fit to such a binding model. These data show that at pH 6.0, 2AT exhibits binding behavior with respect to W191G that is similar in nature to that observed for protonated imidazolium (Fitzgerald et al., 1995), but with a 4-fold higher affinity. These experiments suggested that 2AT specifically binds to the cavity formed by deletion of the Trp-191 side chain with reasonably good affinity.

Direct evidence for the binding of this compound to the W191G mutant was obtained by X-ray crystal structure determination. A complete data set extending to 2.3 Å resolution (Table 1) was collected from two crystals of W191G after soaking them in 50 mM 2AT at pH 6.0, and an $F_o - F_c$ Fourier omit map was constructed by merging this data set with the structure factor amplitudes and phases obtained from a model (PDB entry 1cmq) that was refined against data for an unsoaked W191G crystal (Fitzgerald et al., 1994). The omit map shown in Figure 3 shows clear

Table 1: Crystallographic Data Statistics^a

	2AT bound W191G	2AT modified W191G
crystal form	mkt	by
unit cell, a, b, c (Å)	105.00, 74.22, 45.33	106.97, 75.76, 50.85
resolution (Å)	2.3	1.70
I/σ_I avg [resolution limits (Å)]	12.08 (2.30–6.30)	24.47 (1.70–19.0)
I/σ_I last shell [resolution limits (Å)]	2.01 (2.26–2.28)	9.6 (1.70–1.86)
no. of reflections	16 531	45 073
completeness (%)	98	96
R_{sym}	0.074	0.040

^a The terms mkt and by refer to crystal forms characterized previously (Fitzgerald et al., 1994). The 2AT-bound W191G data were indexed and integrated using XENGEN (Howard et al., 1985). The 2AT-modified W191G data were indexed and integrated using DENZO (Otwinowski, 1993).

evidence for the electron density of 2AT within the cavity. The molecule binds with a clearly defined orientation, as indicated by the electron density features which were resolved for both the 2-amino substituent and the ring sulfur. Placement of a model for 2AT into this density indicates that the 2-amino substituent is involved in hydrogen bonding interactions with the peptide carbonyl of His-175 and a structural water, HOH-308, which is also conserved in the WT structure. In addition to the 2AT, an additional solvent peak, labeled HOH-401, was observed to hydrogen bond to the 2AT ring nitrogen and carboxylate of Asp-235 within the cavity. The position occupied by HOH-401 is analogous to one of the solvent peaks observed in the structure of the solvent-filled cavity (Fitzgerald et al., 1994). Importantly, the ring sulfur of 2AT was observed to be 3.2 Å from the heme γ -meso-carbon atom, placing it in direct van der Waals contact with the heme cofactor, and ideally positioned for oxidation by this center.

Reaction of 2AT with W191G, W191F, and WT CCP. We have obtained optical and EPR data that strongly suggest that 2AT reduces the oxidized heme center of W191G from within the cavity. The optical spectra of Figure 4A show the reductive titration of the ferryl state of W191G with 2AT. The Soret band of the predominantly low-spin ferric state of W191G, with a λ_{max} of 413 nm, shifts to 420 nm and decreases in intensity 15 s after addition of H_2O_2 , consistent with the partial formation of a ferryl heme species. As shown in Figure 4A, addition of 2AT results in a blue shift of the Soret to 413 nm, indicating reduction of the ferryl to a ferric heme species. It is noted that the intensity of this band is reduced somewhat compared to the starting spectrum. This behavior has been seen for a number of mutants of CCP and may be related to a small amount of protein denaturation accompanying oxidative turnover. The blue shift (observed at pH 6.0) in the W191G ferryl heme Soret did not occur when the above experiment was repeated at pH 4.5, indicating that oxidation of 2AT by W191G does not occur with the cationic form of the ligand ($\text{p}K_a = 5.3$). These results are in sharp contrast to those from similar experiments performed on W191F (Figure 4B). In this case, the low-spin ferric enzyme also undergoes a red shift from 411 to 416 nm upon reaction with H_2O_2 . This is consistent with previous results showing that this mutant forms a transient intermediate similar to Compound I, containing a ferryl/porphyrin radical which decays within 50 ms to give a ferryl species characteristic of Compound II (Erman et al., 1989).

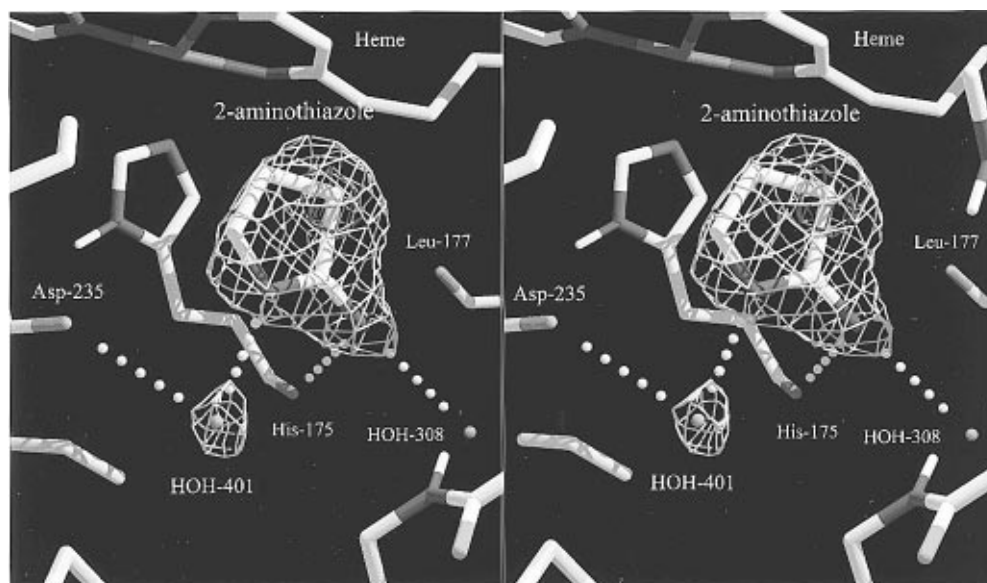


FIGURE 3: Stereoview of a Fourier omit map of W191G soaked in 2-aminothiazole (2AT). Crystals were soaked in artificial mother liquor containing 50 mM 2AT for 1 h prior to data collection. The omit map was calculated as $F_o - F_c$, where the calculated structure factors were derived from a model for W191G which had been refined without containing water or 2AT in the cavity. The map is contoured at $+4\sigma$ (white) and $+9\sigma$ (red). The orientation of the 2AT was indicated by the density attributed to the amino substituent at low contour and the sulfur atom at the high contour level.

However, as addition of 2AT does not result in a blue shift in the Soret, this ferryl species does not appear to be easily reduced by 2AT. Finally, the same experiment done with WT enzyme (Figure 4C) shows that Compound ES, containing the ferryl/Trp radical, is also unreactive toward 2AT.

The EPR spectra shown in Figures 5 and 6 are consistent with the reduction of the ferryl heme of W191G but not WT enzyme by 2AT. In Figure 5, reaction of W191G with 1.2 equiv of H_2O_2 results in the disappearance of the mixed high- and low-spin ferric signals as the iron is oxidized to an EPR silent state. In addition, a narrow isotropic radical is observed at $g = 2.002$ that represents less than 0.1 spin/heme. A similar substoichiometric signal has been reported for mutants of CCP in which the formation of the Trp-191 radical is prevented, and in WT enzyme upon reaction with high concentrations of H_2O_2 (Fishel et al., 1991; Goodin et al., 1986; Hori & Yonetani, 1985). Addition of 15 equiv of 2AT to this oxidized form of W191G results in the complete regeneration of the ferric high- and low-spin signals seen for the starting ferric W191G. In addition, the narrow radical signal is abolished by 2AT addition. It is important to note that no evidence for an additional free radical signal is observed after addition of 2AT, indicating that, if an aminothiazole-based radical is generated, it is not stable enough to be observed under these conditions. These results are in contrast to those observed in Figure 6 for the WT enzyme. In this case, oxidation of the ferric enzyme with H_2O_2 also results in the disappearance of the ferric heme signals as the iron is oxidized to the ferryl state. In addition, the broad signal of the Trp-191 free radical is observed near $g = 2$. This signal is quite distinct in its line shape and relaxation properties from the narrow isotropic signal observed for W191G, and its unusual properties have been characterized in detail (Houseman et al., 1993; Huyett et al., 1995; Sivaraja et al., 1989). At 77 K, these differences are evident only in the broadened wings of the Trp-191 radical relative to the narrow minority signal as previously noted (Hori & Yonetani, 1985). We also note that the low-spin signals observed for the ferric enzyme result from a well-

known freezing artifact that occurs when samples are frozen in the absence of glassing agents such as glycerol (Yonetani & Anni, 1987). Such agents were omitted from all samples in this study to aid in the rapid and uniform mixing required for the 2AT additions. Importantly, addition of 15 equiv of 2AT to the Compound ES state of WT CCP does not result in quantitative reduction of either the ferryl heme or Trp-191 radical. While a partial quenching of the Trp-191 radical is indicated, very little ferric heme is produced by 2AT addition. Thus, 2AT effectively reduces both the ferryl and radical centers of W191G to produce a ferric enzyme but is unreactive toward the analogous inaccessible centers of the WT enzyme.

Covalent Modification by 2AT. We have observed that W191G is covalently modified by 2AT in the presence of H_2O_2 . Attempts to measure steady state turnover of 2AT by W191G were hampered by the inactivation of the enzyme over approximately 1 min in the presence of H_2O_2 and 2AT. The nature of this inactivation was investigated by incubating samples of enzyme, 2AT, and H_2O_2 in a 1:5:20 molar ratio for 3 h at 25 °C and subjecting these reaction mixtures to HPLC analysis. Apoprotein and heme peaks were eluted and analyzed by EMS. Heme extracted from treated samples was observed by EMS to be unmodified. However, as shown in Figure 7B, EMS of W191G apoprotein fractions after reaction with 2AT and H_2O_2 indicated the presence of two species with masses of 33 420 g/mol (± 3 g/mol) and 33 534 g/mol (± 3 g/mol). The lighter component was identical in mass to the single peak which was observed for W191G in the absence of 2AT, with or without H_2O_2 , and compared well with the expected mass of the W191G apoprotein (33 421.5 g/mol). The second component was heavier than this by 114 g/mol and is consistent with the covalent addition of 2AT (100 g/mol) and one oxygen atom and the loss of two protons. This modified form of the enzyme was not observed after incubation of W191G with either 2AT or H_2O_2 individually and thus appeared to be the result of 2AT reaction with the oxidized enzyme. Analysis of similarly incubated WT protein (Figure 7A) gave only a single species

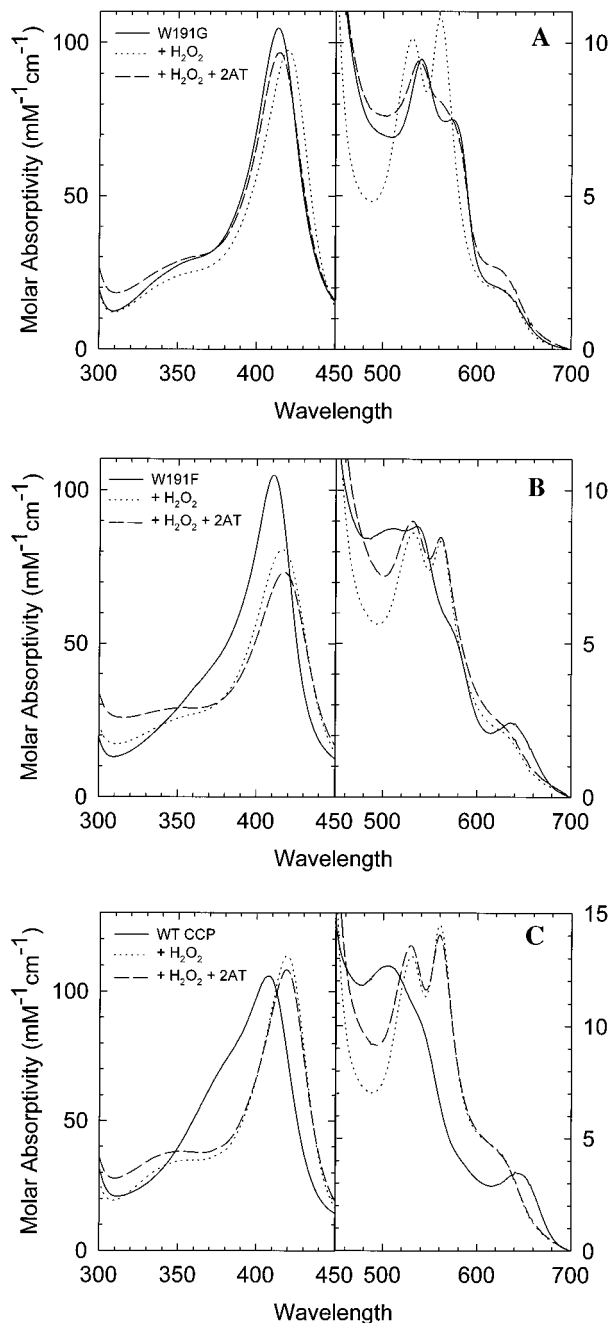


FIGURE 4: UV-vis spectra of W191G (A), W191F (B), and WT (C) in 100 mM phosphate at pH 6.0. Protein concentrations were 10 μ M. Spectra are shown in the ferric state (solid), after addition of a 1.2-fold molar excess of H_2O_2 (dotted), and after the subsequent addition of 100 equiv of 2AT (dashed).

with the expected mass (33 550.6 g/mol) of the unmodified apoprotein (33 550 \pm 3 g/mol observed). A similar incubation was performed with the W191F mutant, which lacks the binding cavity. As Figure 7C shows, two peaks were again observed corresponding to the unmodified apoprotein (33 516 \pm 3 g/mol observed) and a second species (33 630 \pm 3 g/mol) which was 114 mass units heavier than the first. Thus, these data indicate that only the mutants lacking the Trp-191 radical were covalently modified and that the site of modification was distinct from the engineered W191G cavity. Finally, we have observed (data not shown) that W191G/2AT/ H_2O_2 in a ratio of 1:5:1 did not show any evidence of the additional peak observed at higher peroxide ratios. Thus, the extent of the covalent modification was

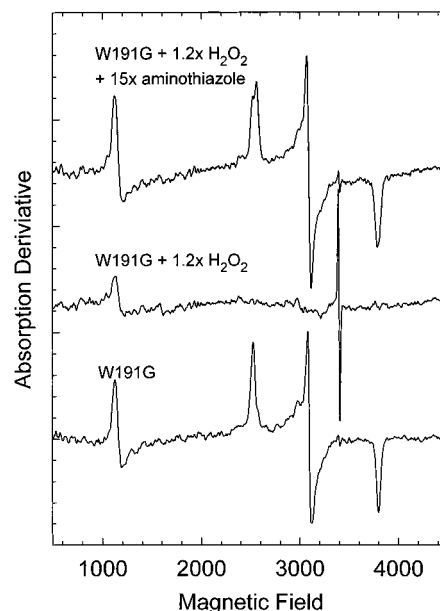


FIGURE 5: EPR spectra of W191G in the ferric (bottom), ferryl (middle), and 2AT-treated ferryl (top) states at 77 K. Spectra were collected in 3 mm OD quartz EPR tubes containing 900 μ M enzyme in 100 mM potassium phosphate buffer at pH 6.0. Spectra were collected with a 9.51 GHz microwave frequency, a 20 mW microwave power, and a 5.0 G modulation amplitude at 100 KHz. (Bottom) The ferric enzyme shows a mixture of high- and low-spin signals. (Middle) After addition of H_2O_2 , the protein is converted to the EPR silent ferryl state. (Top) Addition of 2AT to ferryl W191G results in regeneration of the ferric heme signal and quenching of the isotropic alternate radical signal at $g = 2$.

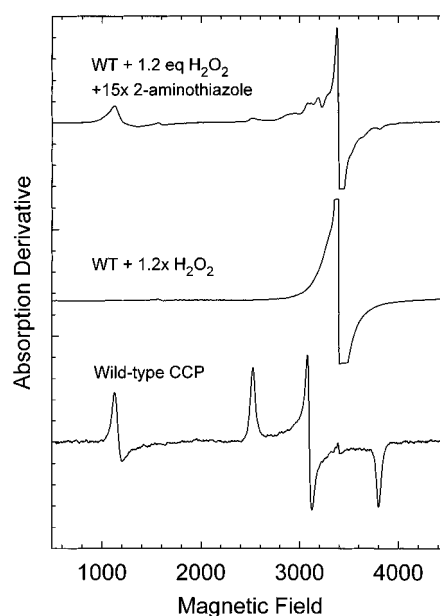


FIGURE 6: EPR spectra of WT in the ferric (bottom), ferryl (middle), and 2AT-treated ferryl (top) states at 77 K. Spectra were collected in 3 mm OD quartz EPR tubes containing 900 μ M enzyme in 100 mM potassium phosphate buffer at pH 6.0. Spectra were collected with a 9.51 GHz microwave frequency, a 20 mW microwave power, and a 5.0 G modulation amplitude at 100 KHz. (Bottom) WT ferric signal. (Middle) After addition of H_2O_2 , the protein is converted to the EPR silent ferryl state. (Top) Addition of 2AT to ferric WT does not result in complete regeneration of the ferric heme signal or in reduction of the Trp-191 radical signal near $g = 2$.

small following a single turnover of the enzyme, indicating that the modification reaction occurred with low efficiency and accumulated over multiple turnovers.

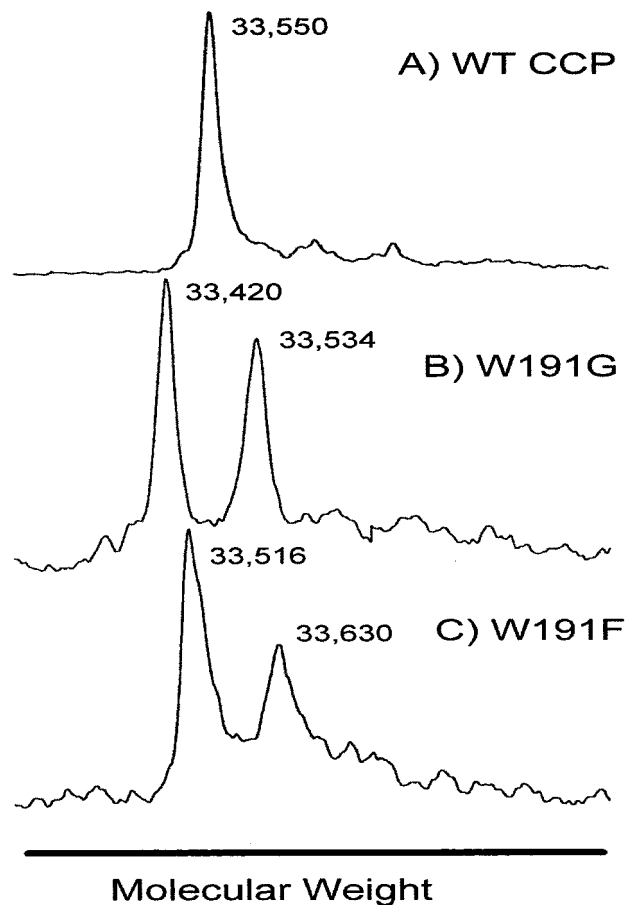


FIGURE 7: Electrospray ionization mass spectra (EMS) of WT (A), W191G (B), and W191F (C) after treatment with 2AT in the presence of H_2O_2 . Five equivalents and 20 equiv of 2AT and H_2O_2 were used, respectively, and the reactions were allowed to proceed over a 3 h period before HPLC/EMS analysis as described in Materials and Methods.

The site on the enzyme modified by 2AT was identified by peptide mapping and sequencing. W191G that had been treated with and without 2AT in the presence of H_2O_2 was digested with CNBr, and the fragments were separated by HPLC (Figure 8) and analyzed by EMS. Each of the major peaks observed for unmodified W191G corresponded to fragments expected for either complete or partial CNBr fragmentation. However, modified W191G gave an additional peak with a retention time of 22.3 min in addition to a nearby fragment eluting at 21.8 min for both samples. For both modified and unmodified samples, the peak eluting at 21.8 min consistently gave a mass of 7319 ± 1 amu which was near the expected mass (7261 amu) of the CNBr fragment from Met-230 to Leu-294. The peak eluting at 22.3 min in the 2AT-treated sample had a mass of 7435 ± 1 amu, or 115 amu greater than the fragment eluting at 21.8 min. Thus, the covalent adduct was localized on the CNBr fragment between Met-230 and Leu-294. Samples of the modified and unmodified CNBr fragments were separately pooled and subjected to automated peptide sequencing. The results of this analysis, summarized in Table 2, revealed that the standard phenylthiohydantoin (PTH) amino acid peak for Tyr-236 was missing only in the modified peptide, and thus, Tyr-236 was identified as the site of covalent modification. A sample of W191F which had been treated with 2AT and H_2O_2 as described above also gave two peaks in the CNBr map with retention times of 21.8 and 22.3 min, indicating

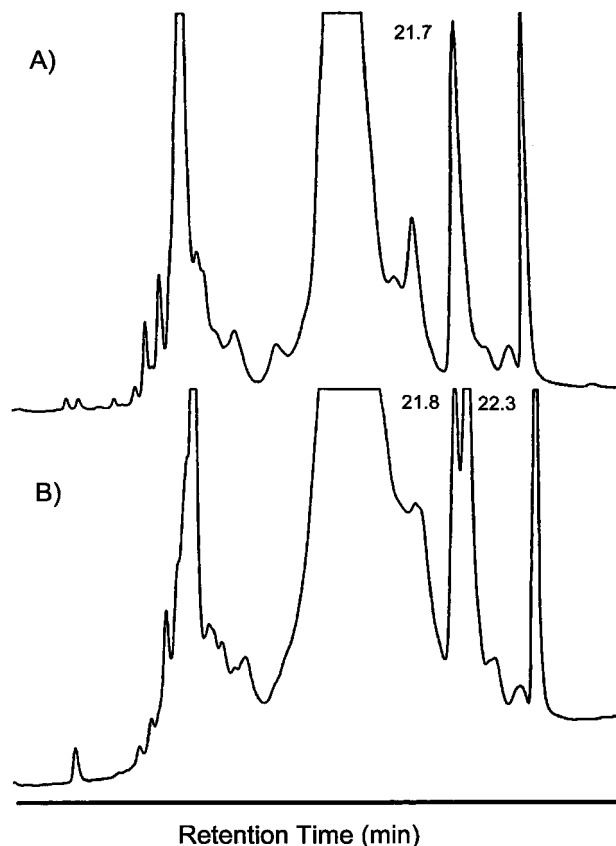


FIGURE 8: Peptide mapping of W191G. (A) CNBr treatment of W191G/ H_2O_2 followed by chromatographic separation of the resulting peptides via C_{18} reversed phase HPLC (see Materials and Methods). (B) As in panel A, except that 2AT was included in the reaction mixture. An additional peak eluting at 22.3 min was observed near the CNBr fragment at 21.7 min corresponding to the Met-230–Leu-294 fragment.

Table 2: Peptide Sequencing Data^a

sample	retention time (min)	mass (Da)	amino acid sequence
W191G + 2AT + H_2O_2	21.8	7319	MPTDYSLIQ
	22.3	7435	MPTD SLIQ
W191G + H_2O_2	21.8	7319	MPTDYSLIQ

^a Amino acid sequencing of the first nine amino acids of the CNBr cleavage fragment from Met-231 to Leu-294 obtained by HPLC separation. Amino acid sequencing was done by automated Edman degradation and was performed at the Scripps core facility. The missing residue for the modified peptide indicates that no standard PTH amino acid appeared in the chromatogram during that sequencing cycle.

that W191F is modified at a similar position as observed for W191G.

An attempt was made to examine this modified residue directly by X-ray crystallography. Single crystals of the W191G protein that had been preincubated with 2AT and H_2O_2 were grown (Table 1). These crystals, when dissolved and analyzed by EMS, showed a heterogeneous composition similar to that shown in Figure 7B, indicating that they were an approximate 50:50 mixture of modified and unmodified protein. A data set which was 96% complete to 1.7 Å resolution, $R_{sym} = 0.040$, was collected at a low temperature (-190 °C) and merged with a similar data set collected on an unmodified W191G crystal. Initial examination of $F_o - F_c$ Fourier difference maps did not show clear evidence for an electron density feature above background that was not accounted for in the model. However, with the knowledge

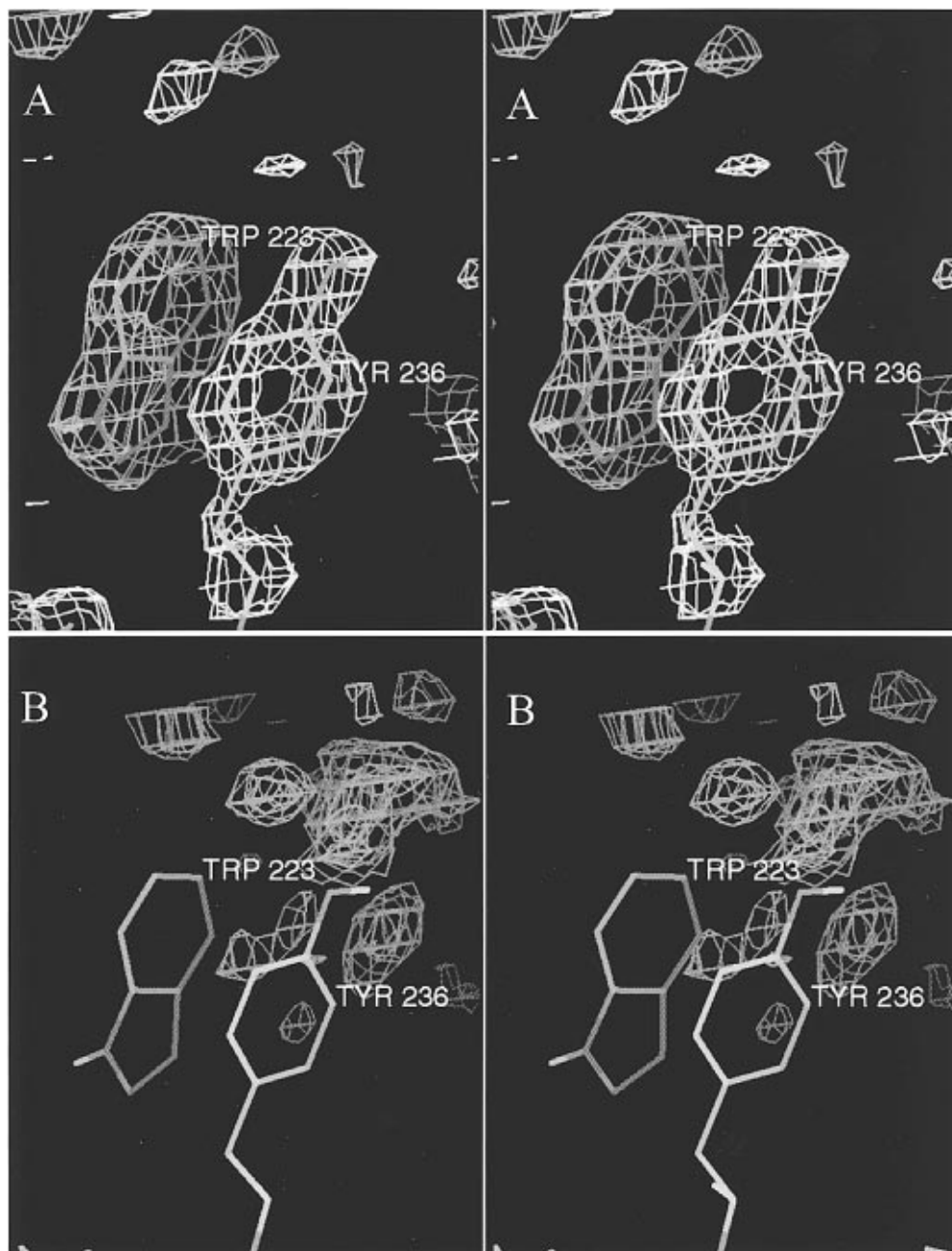


FIGURE 9: Stereoview of a Fourier omit map of 2AT/H₂O₂-treated W191G for data collected to 1.7 Å at -190 °C. The calculated structure factors were derived from a model for W191G which had been refined without containing water or 2AT in the cavity. The $2F_o - F_c$ map (A) is contoured at $+2\sigma$. The $F_o - F_c$ map (B) is contoured at $+4\sigma$ (blue) and -4σ (red).

that Tyr-236 is the site of modification, careful examination of the map in this region (Figure 9) revealed a weak electron density feature that extends from the tyrosyl oxygen of this residue. This density is quite weak, however, possibly due to the heterogeneous nature of the sample, disorder, or both. While it was not possible to identify the group attached to Tyr-236, there is evidence that it is linked via the tyrosyl oxygen.

DISCUSSION

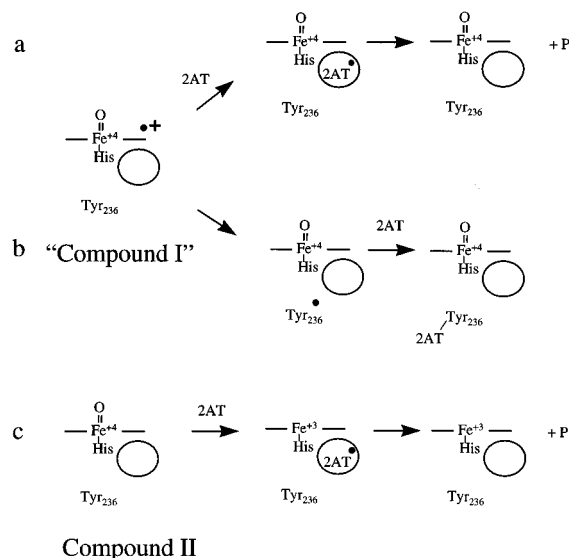
Oxidation of 2AT by the oxidized heme from within the artificial cavity of W191G can be inferred by comparison of the behavior of this mutant with that of W191F and WT CCP. Complete reduction of the ferryl heme was only observed for the W191G mutant, in spite of the fact that W191F and WT both form a ferryl species. The X-ray

crystallographic observation that 2AT binds to the cavity with high affinity at a position that places it in contact with the heme macrocycle provides additional support for the proposed direct reaction with the heme center. Two alternate explanations for the specific reactivity of 2AT with W191G can be made, however. It is possible that the W191G mutant is peculiar in that it forms an oxidized intermediate that has a higher reactivity than that of W191F or WT CCP. However, recent measurements of the Fe⁴⁺/Fe³⁺ reduction potentials by direct voltammetry (F. A. Armstrong, unpublished observations) suggest that the W191G and W191F mutants have similar reduction potentials. Thus, the reactivity displayed by W191G for 2AT does not appear to result from an inherently more reactive ferryl state. It is also possible that reduction of the ferryl heme of W191G occurs through the intermediate reduction of the surface Tyr-236 radical

rather than from within the Trp-191 cavity. However, the W191F mutant has also been observed to form this radical, but is not reduced by 2AT. Direct reduction of the heme center by 2AT when bound to the W191G cavity is thus the only simple model consistent with the above observations.

The characterization of the site at which W191G is covalently modified by 2AT provides an unanticipated assignment of the "alternate" free radical species of CCP that has been the subject of several investigations (Fishel et al., 1991; Hori & Yonetani, 1988; Scholes et al., 1989). In addition to the broad, rapidly relaxing signal from the Trp-191 radical of Compound ES, which accounts for approximately 1 spin per heme, several studies have reported the observation of a narrow isotropic minority signal which typically represents 0.05–0.2 spin per heme in peroxide-oxidized samples (Fishel et al., 1991; Goodin et al., 1986; Hori & Yonetani, 1985). Definitive evidence showing that the broad signal of Compound ES is associated with Trp-191 was provided by electron nuclear double-resonance (ENDOR) measurements of CCP containing isotopically labeled tryptophan (Houseman et al., 1993; Huyett et al., 1995; Sivaraja et al., 1989), but the source of the narrow signal has not been conclusively identified. Its unaltered proton hyperfine coupling in samples containing deuterated tryptophan demonstrates that the narrow signal is not a tryptophan radical (D. Goodin, unpublished observations). The close similarity in the line shapes of this narrow signal and the assigned tyrosine radicals of photosystem II (Barry et al., 1990; Beck & Brudvig, 1987; Debus et al., 1988; Prince, 1988), ribonucleotide reductase (Bender et al., 1989; Larsson et al., 1988; Larsson & Sjoberg, 1986), and prostaglandin H synthase (Karthain et al., 1988; Kulmacz et al., 1990; Picot et al., 1994) is suggestive of a tyrosine radical. However, a number of residues, including Tyr-36, Tyr-42, Tyr-39, Tyr-229, and Tyr-236, were reportedly mutated without definitive conclusions about the identity of this narrow minority signal (Fishel et al., 1991). Evidence indicates that increased amounts of this alternate radical may result from reaction with a transient porphyrin radical intermediate when the formation of the Trp-191 radical is frustrated. It has been observed that peroxide oxidation of W191F results in the transient formation of a ferryl porphyrin π radical similar to Compound I of HRP, but this porphyrin radical quickly decays (within 50 ms) to generate a Compound II-like species (Erman et al., 1989). While it is not certain where this oxidizing equivalent has been deposited, it has also been noted that the narrow EPR signal observed upon oxidation of W191F is about twice as large as that observed for the D235N mutant which may form the Trp-191 radical inefficiently. We have also observed that, if care is taken not to add peroxide in excess, Compound ES of WT CCP can be generated with little or no narrow signal (D. Goodin, unpublished observations). These observations are consistent with an efficient oxidation of Trp-191 by a transient intermediate Compound I for WT CCP, while mutants that prevent formation of the Trp radical result in the persistence of a reactive porphyrin-centered radical resulting in the increased oxidation of another residue. Covalent modification of Tyr-236 by 2AT specifically in the two mutants W191G and W191F identifies this residue as the alternate radical center that has remained unidentified for many years. While the modified Tyr-236 of CCP has not been fully characterized, our results indicate an adduct

Scheme 2



Compound II

near the hydroxyl oxygen, and the mass is consistent with addition of 2AT and possibly one oxygen atom. Reactions between H₂O₂-dependent protein radicals and organic substrates in Mb and Hb (Degray et al., 1997; Dix & Marnett, 1981; Ortiz de Montellano & Catalano, 1985; Reed et al., 1984) may provide some parallels with this reaction.

We propose that 2AT reacts with the oxidized states of W191G by two separate mechanisms, as shown in Scheme 2. Consistent with properties observed for W191F (Erman et al., 1989), we propose that oxidation of W191G by H₂O₂ generates an unstable ferryl porphyrin π radical cation which is short-lived and decays by oxidation of either 2AT or Tyr-236. (Scheme 2, pathways a and b). In pathway b, 2AT quenches the surface accessible radical of Tyr-236 that is formed at low stoichiometry for those mutants that are missing the Trp-191 radical site of WT CCP. This reaction results in the covalent modification of Tyr-236. In a separate reaction (Scheme 2, pathway c), 2AT is observed to reduce the ferryl heme of Compound II to the ferric state. This reaction is only observed for the cavity containing the W191G mutant in which binding of 2AT places the 2AT ring sulfur atom in van der Waals contact with the heme.

CONCLUSION

The results described above allow two principal conclusions to be drawn concerning the interaction of 2AT with the W191G cavity mutant of CCP. First, the gradual covalent modification of Tyr-236 by 2AT provides strong evidence for the assignment of this residue as the minority free radical center that has been observed in CCP for many years. Second, 2AT is observed to bind within the W191G cavity, and its reduction of the ferryl heme center only for this cavity mutant provides compelling evidence that 2AT reduces the ferryl heme of W191G primarily from within the cavity. This demonstrates the successful engineering of a specific unnatural substrate oxidation in an enzyme by cavity complementation.

ACKNOWLEDGMENT

The authors thank Dr. Duncan McRee, Dr. Gary Siuzdak, Dr. Steve Kent, Dr. Yi Cao, Dr. Melissa Fitzgerald, Dr. Michael Fitzgerald, Sheri Wilcox, and Robin Rosenfeld for

helpful discussions and critical reading of the manuscript. We also acknowledge the Lucille P. Markey Charitable Trust, NIH Shared Instrumentation Grant 1 S10 RR07273-01, and the Scripps DNA core facility for technical assistance.

REFERENCES

- Barrick, D. (1994) *Biochemistry* 33, 6546–6554.
- Barry, B. A., Eldeeb, M. K., Sandusky, P. O., & Babcock, G. T. (1990) *J. Biol. Chem.* 265, 20139–20143.
- Beck, W. F., & Brudvig, G. W. (1987) *Biochemistry* 26, 8285–8295.
- Bender, C. J., Sahlin, M., Babcock, G. T., Barry, B. A., Chandrashekar, T. K., Salowe, S. P., Stubbe, J., Lindstrom, B., Petersson, L., Ehrenberg, A., & Sjoberg, B.-M. (1989) *J. Am. Chem. Soc.* 111, 8076–8083.
- Debus, R. J., Barry, B. A., Babcock, G. T., & McIntosh, L. (1988) *Proc. Natl. Acad. Sci. U.S.A.* 85, 427–430.
- Degray, J. A., Gunther, M. R., Tschirret-Guth, R., Ortiz de Montellano, P. R., & Mason, R. P. (1997) *J. Biol. Chem.* 272, 2359–2362.
- Depillis, G. D., Decatur, S. M., Barrick, D., & Boxer, S. G. (1994) *J. Am. Chem. Soc.* 116, 6981–6982.
- Dix, T. A., & Marnett, L. J. (1981) *J. Am. Chem. Soc.* 103, 6744–6746.
- Dolphin, D., Forman, A., Borg, D. C., Fajer, J., & Felton, R. H. (1971) *Proc. Natl. Acad. Sci. U.S.A.* 68, 614–618.
- Eriksson, A. E., Baase, W. A., Wozniak, J. A., & Matthews, B. W. (1992) *Nature* 355, 371–373.
- Erman, J. E., Vitello, L. B., Mauro, J. M., & Kraut, J. (1989) *Biochemistry* 28, 7992–7995.
- Fishel, L. A., Farnum, M. F., Mauro, J. M., Miller, M. A., Kraut, J., Liu, Y. J., Tan, X. L., & Scholes, C. P. (1991) *Biochemistry* 30, 1986–1996.
- Fitzgerald, M. M., Churchill, M. J., McRee, D. E., & Goodin, D. B. (1994) *Biochemistry* 33, 3807–3818.
- Fitzgerald, M. M., Trester, M. L., Jensen, G. M., McRee, D. E., & Goodin, D. B. (1995) *Protein Sci.* 4, 1844–1850.
- Gerfen, G. J., Bellew, B. F., Un, S., Bollinger, J. M., Stubbe, J., Griffin, R. G., & Singel, D. J. (1993) *J. Am. Chem. Soc.* 115, 6420–6421.
- Goodin, D. B., Mauk, A. G., & Smith, M. (1986) *Proc. Natl. Acad. Sci. U.S.A.* 83, 1295–1299.
- Hoganson, C. W., & Babcock, G. T. (1992) *Biochemistry* 31, 11874–11880.
- Hori, H., & Yonetani, T. (1985) *J. Biol. Chem.* 260, 349–355.
- Hori, H., & Yonetani, T. (1988) *Tanpakushitsu Kakusan Koso* 33, 2965–2972.
- Houseman, A. L. P., Doan, P. E., Goodin, D. B., & Hoffman, B. M. (1993) *Biochemistry* 32, 4430–4443.
- Howard, A. J., Nielson, C., & Xuong, N. H. (1985) in *Methods in Enzymology* (Wyckoff, H. W., Hirs, C. H. W., & Timasheff, S. N., Eds.) pp 452–472, Academic Press, Inc., Orlando, FL.
- Huyett, J. E., Doan, P. E., Gurbel, R., Houseman, A. L. P., Sivaraja, M., Goodin, D. B., & Hoffman, B. M. (1995) *J. Am. Chem. Soc.* 117, 9033–9041.
- Karthein, R., Dietz, R., Nastainczyk, W., & Ruf, H. H. (1988) *Eur. J. Biochem.* 171, 313–320.
- Kulmacz, R. J., Ren, Y., Tsai, A. L., & Palmer, G. (1990) *Biochemistry* 29, 8760–8771.
- Larsson, A., & Sjoberg, B.-M. (1986) *EMBO J.* 5, 2037–2040.
- Larsson, A., Karlsson, M., & Sjoberg, B.-M. (1988) *J. Mol. Biol.* 203, 17780–17784.
- McRee, D. E. (1992) *J. Mol. Graphics* 10, 44–46.
- McRee, D. E., Jensen, G. M., Fitzgerald, M. M., Siegel, H. A., & Goodin, D. B. (1994) *Proc. Natl. Acad. Sci. U.S.A.* 91, 12847–12851.
- Miller, M. A., Han, G. W., & Kraut, J. (1994) *Proc. Natl. Acad. Sci. U.S.A.* 91, 11118–11122.
- Morton, A., & Mathews, B. W. (1995) *Biochemistry* 34, 8576–8588.
- Morton, A., Baase, W. A., & Mathews, B. W. (1995) *Biochemistry* 34, 8564–8575.
- Ortiz de Montellano, P. R., & Catalano, C. E. (1985) *J. Biol. Chem.* 260, 9265–9271.
- Otwinowski, Z. (1993) in *Proceedings of the CCP4 Study Weekend* (Sawyer, L., Isaacs, N., & Bailey, S., Eds.) pp 56–62, Science and Engineering Research Council, Warrington, U.K.
- Picot, D., Loll, P. J., & Garavito, R. M. (1994) *Nature* 367, 243–249.
- Poulos, T. L., & Finzel, B. C. (1984) *Pept. Protein Rev.* 4, 115–171.
- Prince, R. C. (1988) *Trends Biochem. Sci.* 13, 286–288.
- Reed, G. A., Brooks, E. A., & Eling, T. E. (1984) *J. Biol. Chem.* 259, 5591–5595.
- Scholes, C. P., Liu, Y., Fishel, L. A., Farnum, M. F., Mauro, J. M., & Kraut, J. (1989) *Isr. J. Chem.* 29, 85–92.
- Siuzdak, G. (1994) *Proc. Natl. Acad. Sci. U.S.A.* 91, 11290–11297.
- Sivaraja, M., Goodin, D. B., Smith, M., & Hoffman, B. M. (1989) *Science* 245, 738–740.
- Warncke, K., Babcock, G. T., & Mccracken, J. (1994) *J. Am. Chem. Soc.* 116, 7332–7340.
- Yonetani, T. (1976) in *Enzymes* (Boyer, P. D., Ed.) pp 345–361, Academic Press, San Diego.
- Yonetani, T., & Anni, H. (1987) *J. Biol. Chem.* 262, 9547–9554.

BI9708038